07

High-frequency modulation of a quantum dot microring laser at elevated temperature

© A.E. Zhukov[1], E.I. Moiseev[1], I.S. Makhov[1], I.S. Fedosov[1], F.I. Zubov[2], A.M. Mozharov[2], K.A. Ivanov[1], A.M. Nadtochiy[1], N.V. Kryzhanovskaya[1]

[1] HSE University, St. Petersburg, Russia
[2] Alferov Federal State Budgetary Institution of Higher Education and Science Saint Petersburg National Research Academic University of the Russian Academy of Sciences, St. Petersburg, Russia
E-mail: zhukale@gmail.com

Received June 10, 2025
Revised July 14, 2025
Accepted July 15, 2025

Dynamic characteristics of a microring laser with InGaAs/GaAs quantum dots were studied using small-signal high-frequency direct modulation at 55 °C. The largest modulation bandwidth was measured to be 3.7 GHz, the energy-to-data ratio was estimated as 4.2–6.4 pJ/bit. Temperature dependences of the parameters affecting the speed (*K*-factor, threshold current, modulation current efficiency factor) were also determined.

Keywords: high-frequency modulation, microlaser, quantum dots.

DOI: 10.61011/TPL.2025.10.62120.20402

Microdisk/microring cavities based on quantum dots (QDs) are promising for creating compact laser diodes and integrating them with silicon electronics [1,2]. One of their promising applications is using them for optical data transmission on a chip, which places quite high demands on their ability for high-speed operation. Study [3] has demonstrated for a microring laser 50μm in diameter with InAs QDs a room-temperature modulation bandwidth of 6.5 GHz (at the level of −3 dB) at the modulation efficiency of 0.38 GHz/mA$^{1/2}$, and also optical data transmission with the rate of 10 Gb/s. Similar values were obtained at room temperature for an InGaAs-QD-based microdisk laser 23 μm in diameter [4]: modulation bandwidth of 6.7 GHz, data transfer rate of 12.5 Gb/s. In [5], the highest modulation frequency at the −3 dB level for a microring InAs QD laser 50 μm in diameter was 7.5 GHz at the bias current of 22 mA, while the achieved optical transmission rate was 15 Gb/s.

Since optoelectronic devices integrated with silicon electronics are expected to operate at high temperatures, it is important to maintain their serviceability also in this mode. While stripe QD lasers have long demonstrated the ability for high-speed data transmission at the temperatures of at least up to 85 °C [6], studies on the high-temperature speed performance of QD disk/ring microlasers are not available, although such microlasers with continuous pumping have demonstrated lasing at temperatures above 100 °C [7]. In this study, we have examined high-frequency characteristics of a microring laser with InGaAs QDs at 55 °C and showed that the modulation bandwidth at the −3 dB level exceeds 2 GHz in a wide range of forward bias currents, modulation efficiency near the threshold is 1.5 GHz/mA$^{1/2}$, and maximum modulation bandwidth amounts up to 4 GHz.

The laser heterostructure was grown by low-pressure metal-organic vapor-phase epitaxy on an n^+-GaAs substrate misoriented from plane (100) by 6°. The active region contained five QD rows formed by depositing eight $In_{0.4}Ga_{0.6}As$ monolayers [8] separated from each other by GaAs interlayers (40 nm) and placed in the middle of a 0.8 μm thick GaAs waveguide bounded by the $Al_{0.34}Ga_{0.66}As$ emitters. Ring cavities with the outer/inner diameter of 20/6 μm were fabricated by photolithography and dry etching to the depth of 5 μm (see the inset to Fig. 1). The ring p-contact to the top p^+-GaAs layer was formed by metallization of AgMn/Ni/Au. The microrings were then planarized with the SU8 epoxy resist; on top of the resist, gold contact pads 50 × 90 μm in size were fabricated, to which 50 μm

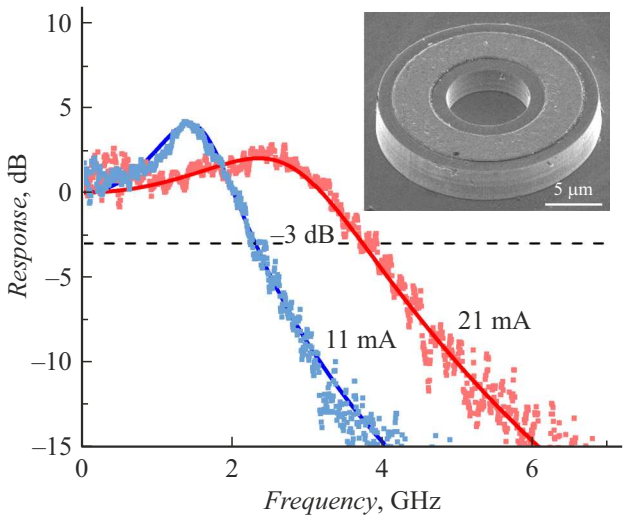

Figure 1. AFRs at 55 °C for different direct current values. Symbols represent experimental data, the dashed line illustrates approximation via relation (1). The inset presents a microphotograph of a ring cavity with a top contact prior to planarization.

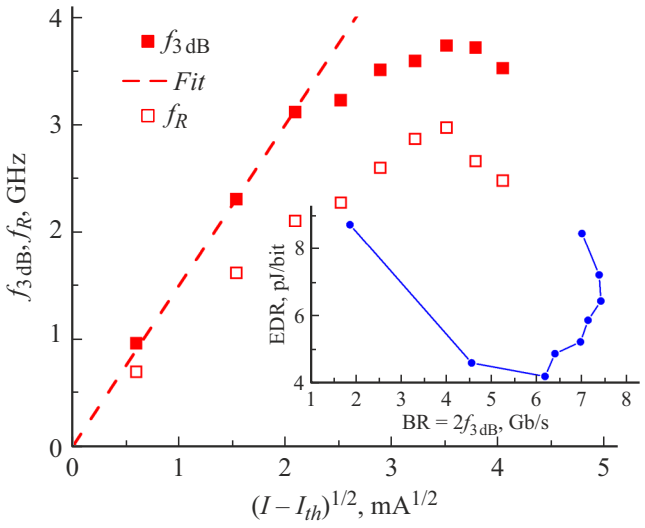

Figure 2. Dependences of the modulation bandwidth (filled symbols) and frequency of relaxation oscillations (open symbols) on the forward bias current at 55 °C. The line corresponds to the modulation efficiency of 1.5 GHz/mA$^{1/2}$. The inset presents the calculated energy-to-data ratio.

thick gold contact wire was connected. On the side of substrate, a continuous AuGe/Ni/Au *n*-contact was made. The punctured chip containing the microlaser was soldered substrate-side down onto a holder placed on a copper heat sink.

The radiation was collected laterally by using a fiber-coupled long-focus objective ×20 Mitutoyo NIR with the numerical aperture of 0.4. In the static mode, emission spectra were recorded using spectral analyzer Yokogawa AQ6370C (with the spectral resolution of 0.2 nm). The threshold current at 55 °C was 8.6 mA. The lasing wavelength was 1105 nm. The spectrum had a quasi-single-frequency character: at the pump current equal to doubled threshold current, the side mode suppression coefficient was 25 dB. Dynamic characteristics were investigated in the frequency range up to 20 GHz by using a high-speed detector (New Focus 1434 25 GHz) and circuit analyzer (Agilent E8364B). For pumping, a high-frequency ground-signal-ground (GSG) probe was used. A modulation signal with a certain frequency of f was supplied through a high-frequency tee-joint together with forward-bias direct current I set by source-measure unit Keithley 2401. Amplitude-frequency responses (AFRs) were measured at various bias currents, and, concurrently, voltage drop across the laser diode was measured. The holder temperature was maintained at 55 °C by using a feedback resistive heater.

Fig. 1 demonstrates AFRs measured at 55 °C at two different forward bias currents. In the considered range of currents (from the threshold value up to 23 mA), relaxation oscillations remain incompletely damped, as evidenced by a pronounced resonance peak. The experimental data were used to estimate the modulation bandwidth defined as frequency $f_{3\,dB}$ at which the response drops by −3 dB with respect to its low-frequency value. Evidently, at 55 °C the modulation bandwidth exceeds 2 GHz in a wide range of bias currents (Fig. 2). Near threshold current I_{th}, frequency $f_{3\,dB}$ may be approximated by function $f_{3\,dB} = \mathrm{MCEF}\sqrt{I - I_{th}}$, where MCEF is the modulation current efficiency factor [9] determined as 1.5 GHz/mA$^{1/2}$. With a further increase in the bias current, the modulation band growth slows down; then $f_{3\,dB}$ decreases. The largest modulation bandwidth was 3.73 GHz (at the current of 21 mA). The error-free optical data transmission rate BR is proportional to frequency $f_{3\,dB}$, namely $\mathrm{BR} = Mf_{3\,dB}$, where coefficient M is about 2. For instance, in [4] this coefficient for a microdisk laser was $12.5/6.7 = 1.87$, while [10] reported for high-speed vertical-cavity lasers the M values ranging from 1.7 to 2.46. Therefore, we may assume that quantum-dot microring lasers will be able to realize data transmission at the temperature elevated to 55 °C with the rate of about 7 Gb/s. Energy consumption for transmitting one bit (energy-to-data ratio, EDR) was calculated as $\mathrm{EDR} = \frac{UI}{\mathrm{BR}}$, where I is the forward bias current, U is the corresponding electrical voltage, $\mathrm{BR} = 2f_{3\,dB}$ is the expected data transmission rate at $M\bar{2}$. The relationship between EDR and BR is shown in the inset to Fig. 2. The lowest power consumption is estimated as 4.2 pJ/bit at the rate of 6.2 Gb/s and EDR = 6.4 pJ/bit at the highest rate of 7.5 Gb/s.

The experimentally measured small-signal modulation curves were approximated via the relation derived by analyzing the rate equations [11]:

$$A(f) = \frac{f_R^4}{(f_R^2 - f^2)^2 + f^2\left(\frac{\gamma}{2\pi}\right)^2} \frac{1}{1 + \frac{f^2}{f_P^2}}. \qquad (1)$$

As a result, parameters determining the laser speed performance were found for each point of operation: relaxation oscillation frequency (f_R) and relaxation oscillation damping factor (γ), as well as parasitic cutoff frequency (f_P). As found out, the latter does not exhibit a regular dependence on either the bias current or temperature (inset in Fig. 3). The mean and standard deviation determined at 13, 28, and 55 °C are 5.4 ± 0.9, 5.7 ± 1.1, and 5.6 ± 1.2 GHz, respectively. To our mind, the parasitic cutoff is associated with recharging of the microlaser capacitance. The fact that at 55 °C the modulation band appears to be below cutoff frequency f_P indicates that $f_{3\,dB}$ is affected by other speed restriction mechanisms.

Fig. 3 presents the dependence of the relaxation oscillation damping factor on relaxation oscillation frequency and its approximation via expression $\gamma = Kf_R^2 + \gamma_0$ [11]. K-factor was estimated as 1.2 ns, the damping factor low-frequency component caused by the finite lifetime of charge carriers was found to be $\gamma_0 = 3.5$ GHz. Maximum modulation bandwidth $f_{\max}$ limited by damping of relaxation oscillations may be obtained from (1) in the limit $f_P \to \infty$ under the assumption that $A = 1/2$. Frequency $f_{\max}$ is a complex function of parameters K and γ_0 [12], which gets simplified to $f_{\max} \approx \frac{2\sqrt{2}\pi}{K} - \frac{\gamma_0}{2\sqrt{2}\pi}$ when $K\gamma_0/(4\pi^2)$ is small.

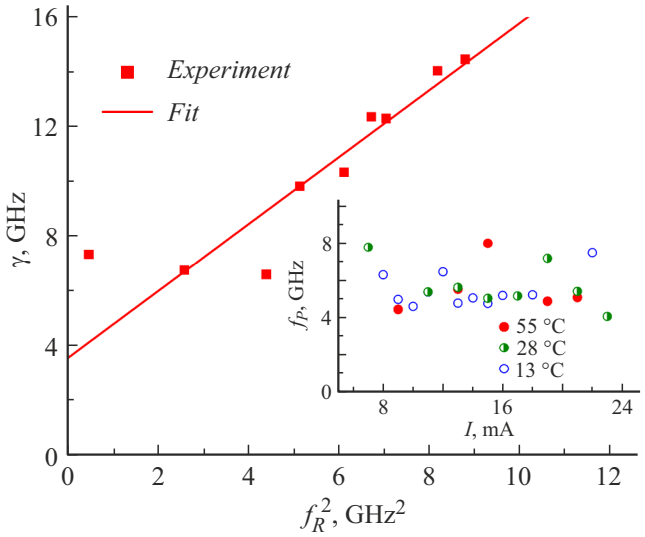

Figure 3. Relationship between the frequency and relaxation oscillation damping factor (symbols) at 55 °C and approximation at $K = 1.2$ ns, $\gamma_0 = 3.5$ GHz. The inset demonstrates the parasitic cutoff frequency versus forward bias current at different temperatures.

For the parameter values we have determined, $f_{\max}$ is 6.8 GHz. Thus, the internal maximum speed performance is almost 2 times higher than the experimentally determined maximum frequency $f_{3\,\mathrm{dB}}$.

Fig. 2 shows the current dependence of relaxation oscillation frequency f_R deduced from the AFR approximation via (1). Evidently, the f_R and $f_{3\,\mathrm{dB}}$ behaviors are qualitatively the same. For instance, the increase in the relaxation oscillation frequency with increasing current gradually slows down; f_R reaches its maximum at the same current as the modulation bandwidth and then decreases. Since the relaxation oscillation frequency itself is not affected by either the damping factor or device capacitance, such behavior indicates, as we believe, a significant influence on the dynamic characteristics from the microlaser self-heating. The increase in the laser operating temperature at high currents is especially characteristic of small-area devices, e.g. vertical-cavity lasers [13] and microdisks [14], since thermal resistance increases with decreasing device size. The temperature increase makes the spontaneous recombination current I_{sp} continue to increase beyond the lasing threshold. This in turn may slowdown the growth of the relaxation oscillation frequency which should be proportional to the square root of the stimulated recombination current, i.e. $f_R \propto \sqrt{I - I_{sp}}$.

In addition, dynamic characteristics of the microring laser were measured at 28 and 13 °C. In the latter case, Peltier cooling was used. As we have already mentioned, the cutoff frequency does not exhibit any regular dependence on temperature. Fig. 4 presents the generalized temperature dependencies of other parameters affecting the speed performance. The threshold current increases significantly with temperature; the dependence may be described by the characteristic temperature of 95 K. The modulation efficiency decreases by approximately 1.5 times as temperature increases from 13 to 55 °C, which, we believe, reflects a decrease in the QD array differential gain at high temperatures. The MCEF decrease due to self-heating may be another factor affecting the modulation bandwidth dependence on current. K-factor remains unchanged within

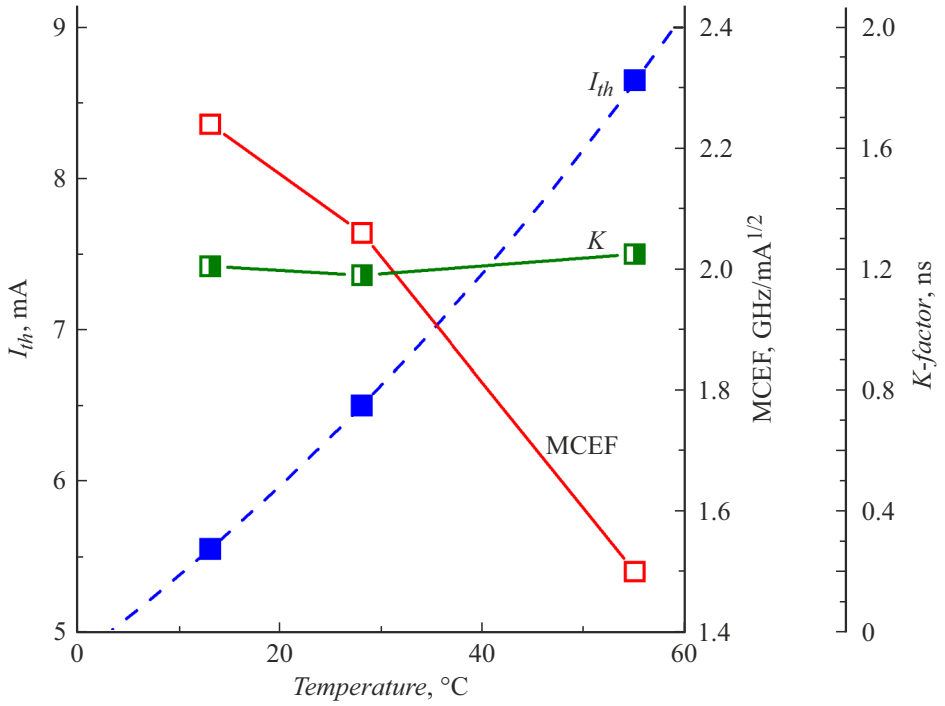

Figure 4. Temperature dependences of the threshold current (I_{th}), modulation current efficiency factor (MCEF) and K-factor.

the error limits of its determination when the temperature varies within the range under consideration. Paper [15] has noted that K-factor of the QD-laser is determined by the sum of the photon lifetime in the cavity and time of carrier capture by the QD state participating in lasing. We may conclude that these times remain virtually unchanged in the temperature range under consideration.

Thus, speed performance of the quantum dot microring laser has been investigated at the holder temperature of 55 °C. The study has shown that the maximum speed performance is significantly affected by the microlaser self-heating leading to the growth slowdown of both the relaxation oscillation frequency and modulation bandwidth. In turn, the self-heating effect on the speed performance may be explained by an increase in the spontaneous recombination current and decrease in the active region differential gain with increasing temperature.

Funding

The study was performed within the framework of the HSE Fundamental Research Program in 2025.

Conflict of interests

The authors declare that they have no conflict of interests.

References

[1] Y. Wan, J. Norman, S. Liu, A. Liu, J.E. Bowers, IEEE Nanotechnol. Mag., **15** (2), 8 (2021). DOI: 10.1109/MNANO.2020.3048094
[2] V. Cao, J.-S. Park, M. Tang, T. Zhou, A. Seeds, S. Chen, H. Liu, Front. Phys., **10**, 839953 (2022). DOI: 10.3389/fphy.2022.839953
[3] Y. Wan, D. Jung, D. Inoue, J.C. Norman, C. Shang, A.C. Gossard, J.E. Bowers, in *2018 Progress in Electromagnetics Research Symp. (PIERS-Toyama)* (IEEE, 2018), p. 249. DOI: 10.23919/PIERS.2018.8598216
[4] F. Zubov, M. Maximov, N. Kryzhanovskaya, E. Moiseev, M. Muretova, A. Mozharov, N. Kaluzhnyy, S. Mintairov, M. Kulagina, N. Ledentsov, Jr., L. Chorchos, N. Ledentstsov, A. Zhukov, Opt. Lett., **44** (22), 5442 (2019). DOI: 10.1364/OL.44.005442
[5] C. Zhang, D. Liang, G. Kurczveil, A. Descos, R. Beausoleil, Optica, **6** (9), 1145 (2019). DOI: 10.1364/OPTICA.6.001145
[6] M.T. Todaro, A. Salhi, L. Fortunato, R. Cingolani, A. Passaseo, M.D. Vittorio, P.D. Casa, F. Ghiglieno, L. Bianco, IEEE Photon. Technol. Lett., **19** (4), 191 (2007). DOI: 10.1109/LPT.2006.890045
[7] E. Moiseev, N. Kryzhanovskaya, M. Maximov, F. Zubov, A. Nadtochiy, M. Kulagina, Yu. Zadiranov, N. Kalyuzhnyy, S. Mintairov, A. Zhukov, Opt. Lett., **43** (19), 4554 (2018). DOI: 10.1364/OL.43.004554
[8] M. Maximov, N. Gordeev, A. Payusov, Yu. Shernyakov, S. Mintairov, N. Kalyuzhnyy, M. Kulagina, A. Nadtochiy, V. Nevedomskiy, A. Zhukov, Laser Phys. Lett., **17** (9), 095801 (2020). DOI: 10.1088/1612-202X/aba0bf
[9] T.R. Chen, B. Zhao, L. Eng, Y.H. Zhuang, J. O'brien, A. Yariv, Electron. Lett., **29** (17), 1525 (1993). DOI: 10.1049/el:19931016
[10] P. Moser, J.A. Lott, G. Larisch, D. Bimberg, J. Lightwave Technol., **33** (4), 825 (2015). DOI: 10.1109/JLT.2014.2365237
[11] L.A. Coldren, S.W. Corzine, M.L. Mašanović, in *Diode lasers and photonic integrated circuits*, 2nd ed. (Wiley, Hoboken, N.J., 2012), p. 261.
[12] Z. Yao, C. Jiang, X. Wang, H. Chen, H. Wang, L. Qin, Z. Zhang, Nanomaterials, **12**, 1058 (2022). DOI: 10.3390/nano12071058
[13] P.P. Baveja, B. Kogel, P. Westbergh, J.S. Gustavsson, A. Haglund, D.N. Maywar, G.P. Agrawal, A. Larsson, Opt. Express, **19** (16), 15490 (2011). DOI: 10.1364/OE.19.015490
[14] A.E. Zhukov, N.V. Kryzhanovskaya, E.I. Moiseev, A.M. Nadtochiy, A.S. Dragunova, M.V. Maximov, F.I. Zubov, S.A. Kadinskaya, Yu. Berdnikov, M.M. Kulagina, S.A. Mintairov, N.A. Kalyuzhnyy, IEEE J. Quantum Electron., **56** (5), 2000908 (2020). DOI: 10.1109/JQE.2020.3009954
[15] M. Ishida, M. Sugawara, T. Yamamoto, N. Hatori, H. Ebe, Y. Nakata, Y. Arakawa, J. Appl. Phys., **101**, 013108 (2007). DOI: 10.1063/1.2407259

Translated by EgoTranslating